Functional derivative approach to Raman response in nonequilibrium many-body systems described by dynamical mean-field theory

O. P. Matveev [1,2] A. M. Shvaika [2] and J. K. Freericks [1]
[1]*Department of Physics, Georgetown University, Washington, DC 20057, USA*
[2]*Yukhnovskii Institute for Condensed Matter Physics of the National Academy of Sciences of Ukraine, Lviv 79011, Ukraine*

(Received 28 July 2025; revised 27 March 2026; accepted 30 April 2026; published 26 May 2026; corrected 30 October 2026)

We employ functional derivatives to calculate spectroscopy in nonequilibrium many-body systems. This allows for all vertex correction effects to be properly incorporated. We focus on electronic Raman scattering. As a concrete example, we present numerical results for the nonresonant contribution to the time-resolved electronic Raman scattering cross section in the A_{1g} symmetry channel solved with dynamical mean-field theory. To do this, we add a small field to the Hamiltonian and take the functional derivative of the "Raman current" operator with respect to this field, which results in an exact expression for the greater Green's function that determines the Raman scattering cross section. This approach avoids the need to set up and solve Bethe-Salpeter equations, which are notoriously difficult to work with in nonequilibrium. We also work out formal expressions for the optical conductivity in the Appendix.

DOI: 10.1103/n17w-5qhk

I. INTRODUCTION

Ultrafast spectroscopy is a powerful tool to probe materials in nonequilibrium [1–5]. The common methodology is the pump-probe protocol: a pump pulse excites the system out of equilibrium and then a probe pulse performs the measurement after a variable time delay. Depending on the frequency and the time profile of the pulses, different excitations can be probed on ultrafast timescales. Strongly correlated materials are of particular interest as they demonstrate such photoinduced phenomena as ultrafast insulator-metal transitions [6–9], melting of charge-ordered phases [10–12] and light-induced superconductivity [13–16]. As an example, Raman scattering spectroscopies allow one to study the low-energy excitations, which provides information about metallic (with a Drude-like peak) or insulating (without a Drude peak) phases. Raman scattering also allows for some symmetry selectivity of the probe when polarizers are used on the incident and scattered light.

From a theoretical point of view, calculating the Raman scattering cross section is challenging already in equilibrium [17,18], while in nonequilibrium it becomes even more difficult. Our work is based on an approach that uses a Green's function technique and the Kadanoff-Baym-Keldysh formalism [19–21]. Raman scattering is determined from two-particle correlation functions, which include vertex corrections responsible for charge screening effects. In nonequilibrium, the vertex correction depends on time and there is no simple way to find it from the conventional Bethe-Salpether equation (as is often done in equilibrium). Instead, one avoids calculating vertex corrections explicitly by using a functional derivative approach where all the vertex corrections are automatically incorporated.

In quantum many-body physics, functional derivatives are used to solve the Dyson equation, where the self-energy is a functional of the Green's function and its functional derivative is the kernel (or vertex) of the Bethe-Salpether equation. This is the origin of so-called conserving approximations [22,23]. In nonequilibrium, this method can be applied to solve the Kadanoff-Baym or Bethe-Salpeter equations [21,24,25]. But it is much easier to just apply the functional derivative method directly to determine the desired response function, rather than the vertex function, because it avoids the need to solve a Bethe-Salpeter equation. This approach can be used in both equilibrium and nonequilibrium cases. It requires finding a connection between the response function one wants to calculate and the functional derivative of an easier to determine function. If one proceeds numerically, as we do here, then one must always work within a fully nonequilibrium formalism even for the equilibrium response, which is why this approach is less common to use for equilibrium problems. Recently, a series of papers on nonequilibrium resonant inelastic x-ray scattering [26–29] and Raman scattering [30] explicitly simulate the probe pulse as a classical light field and take the limit of a weak probe field. Those calculations focus on the impurity response and do not have full momentum resolution of typical experiments. In this paper, we present a step-by-step derivation of the functional derivative method for the calculation of Raman scattering with full momentum resolution. The approach allows the Hamiltonian to have any time dependence, so it is appropriate in both equilibrium and nonequilibrium. Numerically, we evaluate the formalism for the case of Raman scattering in the A_{1g} symmetry channel, because that channel has not yet yielded to other methods in nonequilibrium.

Published by the American Physical Society under the terms of the Creative Commons Attribution 4.0 International license. Further distribution of this work must maintain attribution to the author(s) and the published article's title, journal citation, and DOI.

II. FORMALISM

In optical spectroscopy measurements, the beam of initial photons is directed on the specimen and the number of photons that pass through or are scattered is registered. The total signal contains all contributions, which correspond to the photon absorption and reflection, as well as elastic and inelastic scattering, and can be separated by the experimental setup or data postprocessing.

In equilibrium, the Hamiltonian of an electronic system does not depend on time and in general can be written as

$$\hat{\mathcal{H}} = \hat{\mathcal{H}}_{\rm eq} - \mu \hat{N}, \tag{1}$$

where $\hat{\mathcal{H}}_{\rm eq}$ is the equilibrium electronic Hamiltonian and μ is the chemical potential of the electrons with $\hat{N}$ the total electron number operator. In the Coulomb gauge, the interaction with the electromagnetic field is incorporated by the Peierls' substitution (with $c = 1$)

$$\boldsymbol{p}_i \to \tilde{\boldsymbol{p}}_i(t) = \boldsymbol{p}_i - e\boldsymbol{A}(\boldsymbol{r}_i, t), \tag{2}$$

where $\boldsymbol{A}(\boldsymbol{r}_i)$ is the vector potential value at the electron position $\boldsymbol{r}_i$, plus the instantaneous Coulomb interaction between charges, which usually is already included in the equilibrium Hamiltonian $\hat{\mathcal{H}}_{\rm eq}$. The total Hamiltonian must be supplemented by the electromagnetic field term

$$\hat{\mathcal{H}}_{\rm total} = \tilde{\hat{\mathcal{H}}}(t) + \hat{\mathcal{H}}_{\rm em}, \tag{3}$$

$$\hat{\mathcal{H}}_{\rm em} = \sum_{\boldsymbol{q}\lambda} \omega_{\boldsymbol{q}} a^{\dagger}_{\boldsymbol{q}\lambda} a_{\boldsymbol{q}\lambda}, \tag{4}$$

where the tilde indicates the Peierls' substitution from Eq. (2) has been applied and λ is the summation over the two polarization modes. Below, all derivations will be performed in the interaction representation with respect to the free field Hamiltonian in Eq. (4).

The vector potential contains two contributions from the pump and "probe" $\boldsymbol{A}(\boldsymbol{r}_i, t) = \boldsymbol{A}^{\rm pump}(\boldsymbol{r}_i, t) + \boldsymbol{A}^{\rm probe}(\boldsymbol{r}_i, t)$ (at the moment this auxiliary field is a seed for the future real probe, see below). As a rule, the pump is treated as a classical field with the corresponding electrical field

$$\boldsymbol{E}^{\rm pump}(\boldsymbol{r}_i, t) = -\frac{{\rm d}\boldsymbol{A}^{\rm pump}(\boldsymbol{r}_i, t)}{{\rm d}t}, \tag{5}$$

whereas the "probe" is represented in the interaction representation by the creation ($a^{\dagger}_{\boldsymbol{q}\lambda}$) and annihilation ($a_{\boldsymbol{q}\lambda}$) operators for the photons

$$\boldsymbol{A}^{\rm probe}(\boldsymbol{r}, t) = \sum_{\boldsymbol{q}\lambda} \left(\frac{2\pi}{v\omega_{\boldsymbol{q}}}\right)^{1/2} \boldsymbol{e}^{\lambda}_{\boldsymbol{q}}\, {\rm e}^{{\rm i}\boldsymbol{q}\boldsymbol{r}} \times (a_{\boldsymbol{q}\lambda} {\rm e}^{-{\rm i}\omega_{\boldsymbol{q}} t} + a^{\dagger}_{-\boldsymbol{q}\lambda} {\rm e}^{{\rm i}\omega_{\boldsymbol{q}} t}), \tag{6}$$

where $\boldsymbol{e}^{\lambda}_{\boldsymbol{q}}$ is polarization of the λ mode. In an optical experiment, the magnetic field effects are much smaller (and will be neglected) and we can consider for simplicity the case of the uniform vector potential $\boldsymbol{A}(\boldsymbol{r}_i, t) = \boldsymbol{A}(t)$.

We start with the time-dependent Hamiltonian with the interaction with a time-dependent electric field being described by the Peierls' substitution in the kinetic-energy term. The time-dependent Hamiltonian in momentum space is then given by

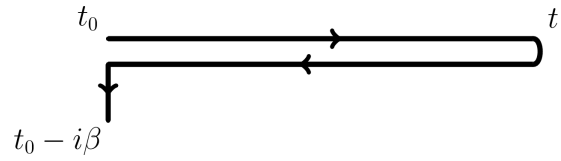


FIG. 1. Kadanoff-Baym-Keldysh time contour. It starts at time t_0, when the system is in equilibrium and the two branches correspond to forward and backward evolution determined by the evolution operators (which first advance in time $\hat{U}$ and then go backwards in time $\hat{U}^{\dagger}$) for the time-dependent operators.

$$\tilde{\hat{\mathcal{H}}}(t) = \sum_{\boldsymbol{k},\sigma} \{\varepsilon(\boldsymbol{k} - e\boldsymbol{A}(t)) - \mu\} \hat{c}^{\dagger}_{\boldsymbol{k},\sigma} \hat{c}_{\boldsymbol{k},\sigma} + \hat{V}(t), \tag{7}$$

where $\varepsilon(\boldsymbol{k})$ is the electronic band structure, $\hat{c}^{\dagger}_{\boldsymbol{k},\sigma}$ ($\hat{c}_{\boldsymbol{k},\sigma}$) are the creation (annihilation) operators of an electron with momentum $\boldsymbol{k}$ and spin σ, and $\hat{V}(t)$ is the potential energy (which can be time dependent). To describe the time evolution in nonequilibrium, we use the Kadanoff-Baym-Keldysh formalism [19,20]. It employs a two-branch time contour in Fig. 1 that is required by the time-evolution operators in the operator expression for the Green's function—all the appropriate two-time-dependent quantities are defined on this contour.

We work on a D-dimension hypercubic lattice with nearest-neighbor hopping only. The bandstructure is given by the sum of cosines for each spatial direction

$$\varepsilon(\boldsymbol{k} - e\boldsymbol{A}(t)) = -\frac{t^*}{\sqrt{D}} \sum_a \cos[k_a - eA_a(t)], \tag{8}$$

where $t^*/\sqrt{D}$ is the hopping energy.

The photon flux of a certain momentum $\boldsymbol{q}_f$, energy ω_f, and polarization $\boldsymbol{e}^f$ is equal to the probability to find it in the final state at infinite time and distance

$$J(\boldsymbol{q}_f, \omega_f) = \sum_n \frac{{\rm e}^{-\beta E_n}}{Z} \langle \Psi_n(\infty) | a^{\dagger}_{\boldsymbol{q}_f, \boldsymbol{e}^f} a_{\boldsymbol{q}_f, \boldsymbol{e}^f} | \Psi_n(\infty) \rangle, \tag{9}$$

where the final state $|\Psi_n(t)\rangle$ results from the time evolution of the initial one, which is a tensor product of the many-body electron state $|n\rangle$ with energy E_n and initial single-photon state $\hat{a}^{\dagger}_{\boldsymbol{q}_i, \boldsymbol{e}^i}|0\rangle$ with momentum $\boldsymbol{q}_i$, energy ω_i, and polarization $\boldsymbol{e}^i$,

$$\begin{aligned} |\Psi_n(t)\rangle &= \tilde{\hat{U}}(t, -\infty) |n\rangle \otimes \hat{a}^{\dagger}_{\boldsymbol{q}_i, \boldsymbol{e}^i} |0\rangle \\ &= \mathcal{T}_t \exp\left[-{\rm i} \int_{-\infty}^{t} {\rm d}\bar{t}\, \tilde{\hat{\mathcal{H}}}(\bar{t})\right] |n\rangle \otimes \hat{a}^{\dagger}_{\boldsymbol{q}_i, \boldsymbol{e}^i} |0\rangle. \end{aligned} \tag{10}$$

In Eq. (9), we have the thermal average over the initial equilibrium many-body electron states and quantum mean value in the vacuum state for photons. Two time-evolution operators $\tilde{\hat{U}}(t, -\infty)$ create a two-branch time contour presented in Fig. 1 in the spirit of the nonequilibrium Kadanoff-Baym-Keldysh formalism [19,20]—all the appropriate time-dependent quantities are defined on this contour.

Next, we expand evolution operator in a series with respect to the probe field

$$\begin{aligned}\tilde{\hat{U}}(t,-\infty) &= \mathcal{T}_t \exp\left[-\mathrm{i}\int_{-\infty}^{t} \mathrm{d}\bar{t}\,\tilde{\hat{\mathcal{H}}}(\bar{t})\right] \approx 1 + \mathrm{i}\int_{-\infty}^{t} \mathrm{d}\bar{t}\,\hat{U}(t,\bar{t})\sum_a \hat{j}_a(\bar{t})A_a^{\mathrm{probe}}(\bar{t})\hat{U}(\bar{t},-\infty)\\ &- \mathrm{i}\int_{-\infty}^{t} \mathrm{d}\bar{t}\hat{U}(t,\bar{t})\,\frac{1}{2}\sum_{a,b}\hat{\gamma}_{a,b}(\bar{t})A_a^{\mathrm{probe}}(\bar{t})A_b^{\mathrm{probe}}(\bar{t})\hat{U}(\bar{t},-\infty)\\ &+ \int_{-\infty}^{t}\mathrm{d}\bar{t}\int_{-\infty}^{\bar{t}}\mathrm{d}\bar{t}'\,\hat{U}(t,\bar{t})\sum_a \hat{j}_a(\bar{t})A_a^{\mathrm{probe}}(\bar{t})\hat{U}(\bar{t},\bar{t}')\sum_b \hat{j}_b(\bar{t}')A_b^{\mathrm{probe}}(\bar{t}')\hat{U}(\bar{t}',-\infty)+\cdots, \end{aligned} \tag{11}$$

where evolution operator $\hat{U}(t,-\infty)$ contains the pump field contribution only and in our further notations we use $\boldsymbol{A}(t) = \boldsymbol{A}^{\mathrm{pump}}(t)$. Here,

$$\hat{j}_a(t) = -\frac{\partial\tilde{\hat{\mathcal{H}}}(t)}{\partial A_a(t)} = e\sum_{\boldsymbol{k},\sigma}\frac{\partial\varepsilon(\boldsymbol{k}-e\boldsymbol{A}(t))}{\partial k_a}\hat{c}^\dagger_{\boldsymbol{k},\sigma}\hat{c}_{\boldsymbol{k},\sigma} \tag{12}$$

is the current operator and

$$\hat{\gamma}_{a,b}(t) = \frac{\partial^2\tilde{\hat{\mathcal{H}}}(t)}{\partial A_a(t)\partial A_b(t)} = e^2\sum_{\boldsymbol{k},\sigma}\frac{\partial^2\varepsilon(\boldsymbol{k}-e\boldsymbol{A}(t))}{\partial k_a\partial k_b}\hat{c}^\dagger_{\boldsymbol{k},\sigma}\hat{c}_{\boldsymbol{k},\sigma} \tag{13}$$

is the stress tensor operator, and we sum over polarizations a and b.

Now, we can substitute this expansion in Eq. (9) and trace out photons by calculating mean values of the photonic factors as

$$\begin{aligned}&\langle 0|\hat{a}_{\boldsymbol{q}_i,\boldsymbol{e}^i}A_{b_1}^{\mathrm{probe}}(t_1')\cdots A_{b_m}^{\mathrm{probe}}(t_m')a^\dagger_{\boldsymbol{q}_f,\boldsymbol{e}^f}a_{\boldsymbol{q}_f,\boldsymbol{e}^f}\\ &\quad\times A_{a_n}^{\mathrm{probe}}(t_n)\cdots A_{a_1}^{\mathrm{probe}}(t_1)\hat{a}^\dagger_{\boldsymbol{q}_i,\boldsymbol{e}^i}|0\rangle_{\mathrm{irr}},\end{aligned} \tag{14}$$

where the time arguments $t_1,\ldots,t_n$ are on the forward branch on the contour and $t_1',\ldots,t_n'$ on the backward one. This expression is nonzero only for an even number of the probe fields. Besides, the contributions from the photons other than the incident (i) or final (f) one on the forward and backward contour branches mutually canceled and only the connected (irreducible) terms contribute. The zero-order contribution is equal to

$$\langle 0|\hat{a}_{\boldsymbol{q}_i,\boldsymbol{e}^i}a^\dagger_{\boldsymbol{q}_f,\boldsymbol{e}^f}a_{\boldsymbol{q}_f,\boldsymbol{e}^f}\hat{a}^\dagger_{\boldsymbol{q}_i,\boldsymbol{e}^i}|0\rangle_{\mathrm{irr}} = \delta_{\boldsymbol{q}_i,\boldsymbol{q}_f}\delta_{\boldsymbol{e}^i,\boldsymbol{e}^f}, \tag{15}$$

corresponding to elastic reflection.

Within the first lowest-order contributions we have

$$\begin{aligned}&\langle 0|\hat{a}_{\boldsymbol{q}_i,\boldsymbol{e}^i}A_{b_1}^{\mathrm{probe}}(t_1')a^\dagger_{\boldsymbol{q}_f,\boldsymbol{e}^f}a_{\boldsymbol{q}_f,\boldsymbol{e}^f}A_{a_1}^{\mathrm{probe}}(t_1)\hat{a}^\dagger_{\boldsymbol{q}_i,\boldsymbol{e}^i}|0\rangle_{\mathrm{irr}}\\ &= \frac{2\pi}{v\omega_{\boldsymbol{q}_f}}e^f_{a_1}e^f_{b_1}\mathrm{e}^{\mathrm{i}\omega_{q_f}(t_1-t_1')}\\ &\quad\times\langle 0|\hat{a}_{\boldsymbol{q}_i,\boldsymbol{e}^i}a_{\boldsymbol{q}_f,\boldsymbol{e}^f}a^\dagger_{\boldsymbol{q}_f,\boldsymbol{e}^f}a_{\boldsymbol{q}_f,\boldsymbol{e}^f}a^\dagger_{\boldsymbol{q}_f,\boldsymbol{e}^f}\hat{a}^\dagger_{\boldsymbol{q}_i,\boldsymbol{e}^i}|0\rangle_{\mathrm{irr}}\\ &= 0,\end{aligned} \tag{16}$$

which corresponds to the spontaneous emission of photons, also known as thermal (or blackbody) radiation, without involving the incident photon and it is reducible. Another contribution is of the type

$$\begin{aligned}&\langle 0|\hat{a}_{\boldsymbol{q}_i,\boldsymbol{e}^i}a^\dagger_{\boldsymbol{q}_f,\boldsymbol{e}^f}a_{\boldsymbol{q}_f,\boldsymbol{e}^f}A_{a_2}^{\mathrm{probe}}(t_2)A_{a_1}^{\mathrm{probe}}(t_1)\hat{a}^\dagger_{\boldsymbol{q}_i,\boldsymbol{e}^i}|0\rangle_{\mathrm{irr}}\\ &= \frac{2\pi}{v\sqrt{\omega_{\boldsymbol{q}_i}\omega_{\boldsymbol{q}_i}}}\langle 0|\hat{a}_{\boldsymbol{q}_i,\boldsymbol{e}^i}a^\dagger_{\boldsymbol{q}_f,\boldsymbol{e}^f}a_{\boldsymbol{q}_f,\boldsymbol{e}^f}\\ &\quad\times\left(e^f_{a_2}a^\dagger_{\boldsymbol{q}_f\boldsymbol{e}^f}\mathrm{e}^{\mathrm{i}\omega_{q_f}t_2}\,e^i_{a_1}a_{\boldsymbol{q}_i\boldsymbol{e}^i}\mathrm{e}^{-\mathrm{i}\omega_{q_i}t_1}\right.\\ &\quad\left.+\,e^i_{a_2}a_{\boldsymbol{q}_i\boldsymbol{e}^i}\mathrm{e}^{-\mathrm{i}\omega_{q_i}t_2}\,e^f_{a_1}a^\dagger_{\boldsymbol{q}_f\boldsymbol{e}^f}\mathrm{e}^{\mathrm{i}\omega_{q_f}t_1}\right)\hat{a}^\dagger_{\boldsymbol{q}_i,\boldsymbol{e}^i}|0\rangle_{\mathrm{irr}}\\ &= \delta_{\boldsymbol{q}_i,\boldsymbol{q}_f}\delta_{\boldsymbol{e}^i,\boldsymbol{e}^f}\frac{2\pi}{v\omega_{\boldsymbol{q}_i}}e^i_{a_1}e^i_{a_2}\\ &\quad\times[\mathrm{e}^{\mathrm{i}\omega_{q_i}(t_2-t_1)}s(t_1,t_p)+\mathrm{e}^{\mathrm{i}\omega_{q_i}(t_1-t_2)}s(t_2,t_p)],\end{aligned} \tag{17}$$

which contributes in elastic scattering and corresponds to photon absorption. Here, the contraction (pairing) of the incident photon with the auxiliary one is spanned in time by the probe pulse represented by the probe envelope function

$$s(t,t_p) = \frac{1}{\sigma_b\sqrt{\pi}}\mathrm{e}^{-(t-t_p)^2/\sigma_b^2}, \tag{18}$$

with t_p the time delay of the probe pulse with respect to the pump pulse. A similar expression can be written for the backward contour branch too.

The lowest-order contributions to inelastic scattering come from the quadratic terms in the evolution operators for both forward and backward contour branches and there are four of them. The nonresonant contribution involves terms with the stress tensor only [from the second row in Eq. (11)], the resonant one involves current operators only [from the last row in Eq. (11)], and the mixed one involves both of them. For the nonresonant inelastic (Raman) scattering we get

$$\begin{aligned}J_N(\omega_i,\omega_f) &= \int_{-\infty}^{+\infty}\mathrm{d}\bar{t}\int_{-\infty}^{+\infty}\mathrm{d}\bar{t}'\sum_{aba'b'}\sum_n\frac{\mathrm{e}^{-\beta E_n}}{Z}\langle n|\hat{U}(-\infty,\bar{t}')\hat{\gamma}_{a',b'}(\bar{t}')\hat{U}(\bar{t}',\bar{t})\hat{\gamma}_{a,b}(\bar{t})\hat{U}(\bar{t},-\infty)|n\rangle\\ &\quad\times\frac{1}{4}\langle 0|\hat{a}_{\boldsymbol{q}_i,\boldsymbol{e}^i}A_{a'}^{\mathrm{probe}}(\bar{t}')A_{b'}^{\mathrm{probe}}(\bar{t}')a^\dagger_{\boldsymbol{q}_f,\boldsymbol{e}^f}a_{\boldsymbol{q}_f,\boldsymbol{e}^f}A_a^{\mathrm{probe}}(\bar{t})A_b^{\mathrm{probe}}(\bar{t})\hat{a}^\dagger_{\boldsymbol{q}_i,\boldsymbol{e}^i}|0\rangle_{\mathrm{irr}}\\ &= \frac{4\pi^2}{v^2\omega_i\omega_f}R_N(\omega_i-\omega_f),\end{aligned} \tag{19}$$

with inelastic scattering cross section

$$R_N(\omega_i-\omega_f)=\int_{-\infty}^{+\infty}\mathrm{d}\bar{t}\int_{-\infty}^{+\infty}\mathrm{d}\bar{t}'\langle\hat{U}(-\infty,\bar{t}')\hat{\tilde{\gamma}}(\bar{t}')\hat{U}(\bar{t}',\bar{t})\hat{\tilde{\gamma}}(\bar{t})\hat{U}(\bar{t},-\infty)\rangle_0 \mathrm{e}^{\mathrm{i}(\omega_f-\omega_i)(\bar{t}-\bar{t}')}s(\bar{t},t_p)s(\bar{t}',t_p)$$
$$=\int_{-\infty}^{+\infty}\mathrm{d}\bar{t}\int_{-\infty}^{+\infty}\mathrm{d}\bar{t}'\langle\hat{\tilde{\gamma}}(\bar{t}')\hat{\tilde{\gamma}}(\bar{t})\rangle_c\,\mathrm{e}^{\mathrm{i}(\omega_f-\omega_i)(\bar{t}-\bar{t}')}s(\bar{t},t_p)s(\bar{t}',t_p), \tag{20}$$

where $\langle\hat{O}\rangle_0$ is the ensemble average of the operator $\hat{O}$ over the initial equilibrium thermal state. Finally, we find that the nonresonant contribution is determined by the correlation function (the greater Green's function) built on the two operators

$$\hat{\tilde{\gamma}}(t)=\sum_{a,b}e_a^i e_b^f\hat{\gamma}_{a,b}(t), \tag{21}$$

which are the convolution of the stress tensor with the polarization vectors, and similar expressions can be written for the resonant and mixed contributions.

For the hypercubic lattice with nearest-neighbor hopping Eq. (8), it is well known [31–33] that within the dynamical mean-field theory ($D\to\infty$ limit) the Raman response for the B_{2g} symmetry contains only resonant contributions, for the B_{1g} symmetry contains resonant and nonresonant contributions, and for the A_{1g} symmetry we have all contributions—nonresonant, resonant, and mixed—and these conclusions hold in nonequilibrium too. Specifically for the nonresonant scattering, the B_{1g} response contains only bare bubble contributions and its time-resolved spectra were analyzed in Ref. [34]. The nonresonant A_{1g} Raman response contains the full bubble renormalization and one has to know the irreducible charge vertex to solve the Bethe-Salpeter equation, which is unknown and one has to find a different approach.

For the A_{1g} symmetry with $\boldsymbol{e}^i=\boldsymbol{e}^f=(1,1,\ldots)$ [31,32] and the band energy in Eq. (8), the stress tensor in Eq. (21) is equal to

$$\hat{\gamma}_{A_{1g}}(t)=\sum_{a,b}e_a^i e_b^f\hat{\gamma}_{a,b}(t)$$
$$=e^2\sum_{\boldsymbol{k},\sigma}\frac{t^*}{\sqrt{D}}\sum_a\cos[k_a-eA_a(t)]\hat{c}^\dagger_{\boldsymbol{k},\sigma}\hat{c}_{\boldsymbol{k},\sigma}$$
$$=-e^2\sum_{\boldsymbol{k},\sigma}\varepsilon(\boldsymbol{k}-e\boldsymbol{A}(t))\hat{c}^\dagger_{\boldsymbol{k},\sigma}\hat{c}_{\boldsymbol{k},\sigma}, \tag{22}$$

which means it is the negative of the hopping term and its mean value [for simplicity, we drop index A_{1g} and use $\hat{\gamma}(t)=\hat{\gamma}_{A_{1g}}(t)$]

$$\langle\hat{\gamma}(t)\rangle=-\mathrm{i}e^2\sum_{\boldsymbol{k},\sigma}\varepsilon(\boldsymbol{k}-e\boldsymbol{A}(t))G^<_{\boldsymbol{k},\sigma}(t,t) \tag{23}$$

is, up to a charge factor, the negative kinetic energy. The momentum-dependent lesser Green's function is defined as follows,

$$G^<_{\boldsymbol{k},\sigma}(t,t')=\mathrm{i}\frac{1}{Z}\mathrm{Tr}\{\mathrm{e}^{-\beta\hat{\mathcal{H}}}\hat{c}^\dagger_{\boldsymbol{k},\sigma}(t')\hat{c}_{\boldsymbol{k},\sigma}(t)\}, \tag{24}$$

where $\hat{\mathcal{H}}$ corresponds to the equilibrium Hamiltonian in Eq. (1). At equal times, $t=t'$ the lesser Green's is proportional to the expectation value of the momentum-dependent number operator $\hat{n}_{\boldsymbol{k},\sigma}(t)=\hat{c}^\dagger_{\boldsymbol{k},\sigma}(t)\hat{c}_{\boldsymbol{k},\sigma}(t)$.

Equation (23) implies that we can treat it as a "Raman current" and calculate the Raman scattering response function by taking a single functional derivative as a typical Kubo response function. For an optical conductivity calculation, one has to add a small virtual field $\delta\boldsymbol{A}(t')$ that is conjugate to the current operator and take the functional derivative of its mean value with respect to this field (see the Appendix for more details). Here, the strategy is as follows. We add a small virtual field $\delta B(t)$ conjugated to the kinetic term in the Hamiltonian and take a functional derivative with respect to this field at some time t'. Then we take the limit $\delta B(t')\to 0$. It should be noted that we add this virtual field to the lattice problem, which correctly accounts for all screening and retardation effects. To demonstrate that this strategy works, we apply it to the Falicov-Kimball model [35] as an example. This model has an exact solution within dynamical mean-field theory (DMFT) that also holds in nonequilibrium [36]. The time-dependent Hamiltonian with a small shift of the kinetic term is given by the following,

$$\hat{\mathcal{H}}(t)=\sum_j\left[U\hat{n}_j^d\hat{n}_j^f-\mu\left(\hat{n}_j^d+\hat{n}_j^f\right)\right]$$
$$+[1+\delta B(t)]\sum_{\boldsymbol{k}}\varepsilon(\boldsymbol{k}-e\boldsymbol{A}(t))\hat{n}^d_{\boldsymbol{k}}, \tag{25}$$

where $\hat{n}_j^d=\hat{d}_j^\dagger\hat{d}_j$ and $\hat{n}_j^f=\hat{f}_j^\dagger\hat{f}_j$ are d- and f-particle number operators on site j, respectively, and $\hat{n}^d_{\boldsymbol{k}}=\hat{d}^\dagger_{\boldsymbol{k}}\hat{d}_{\boldsymbol{k}}$ is d-particle number operator in momentum space. The evolution operator $\hat{U}(t,-\infty)$ becomes

$$\hat{U}(t,-\infty)=\mathcal{T}_t\exp\left\{-\mathrm{i}\int_{-\infty}^t\mathrm{d}\bar{t}\left[\sum_j\left[U\hat{n}_j^d\hat{n}_j^f-\mu\left(\hat{n}_j^d+\hat{n}_j^f\right)\right]\right.\right.$$
$$\left.\left.+[1+\delta B(\bar{t})]\sum_{\boldsymbol{k}}\varepsilon(\boldsymbol{k}-e\boldsymbol{A}(\bar{t}))\hat{n}^d_{\boldsymbol{k}}\right]\right\}. \tag{26}$$

The functional derivative of the average of the stress tensor operator with respect to the small field $B(t')$ with time ordering $t'<t$ is equal to

$$\frac{\delta\langle\hat{\gamma}(t)\rangle}{\delta B(t')}=-\frac{1}{Z}\mathrm{Tr}\left\{\mathrm{e}^{-\beta\hat{\mathcal{H}}_{\mathrm{FK}}}\sum_{\boldsymbol{k}}\varepsilon(\boldsymbol{k}-e\boldsymbol{A}(t))\right.$$
$$\times\left(\frac{\delta\hat{U}^\dagger(t,-\infty)}{\delta B(t')}\hat{n}^d_{\boldsymbol{k}}\hat{U}(t,-\infty)\right.$$
$$\left.\left.+\hat{U}^\dagger(t,-\infty)\hat{n}^d_{\boldsymbol{k}}\frac{\delta\hat{U}(t,-\infty)}{\delta B(t')}\right)\right\}, \tag{27}$$

where $\hat{\mathcal{H}}_{\rm FK}$ is time-independent part of the Hamiltonian in Eq. (25). The derivative of the evolution operators "pulls down" the kinetic energy term from the Hamiltonian, which forms the stress tensor operator as follows,

$$\begin{aligned}\frac{\delta\hat{U}(t,-\infty)}{\delta B(t')} &= \hat{U}(t,t'+\delta t)\frac{\delta\hat{U}(t'+\delta t,t'-\delta t)}{\delta B(t')}\hat{U}(t'-\delta t,-\infty)|_{\delta t\to 0}\\ &= \hat{U}(t,t'+\delta t)\left(-\mathrm{i}\int_{t'-\delta t}^{t'+\delta t}\mathrm{d}\bar{t}\sum_{\boldsymbol{k}}\varepsilon(\boldsymbol{k}-e\boldsymbol{A}(\bar{t}))\hat{n}^d_{\boldsymbol{k}}\delta(\bar{t}-t')\right)\hat{U}(t'-\delta t,-\infty)|_{\delta t\to 0}\\ &= -\mathrm{i}\hat{U}(t,t')\sum_{\boldsymbol{k}}\varepsilon(\boldsymbol{k}-e\boldsymbol{A}(t'))\hat{n}^d_{\boldsymbol{k}}\hat{U}(t',-\infty),\\ \frac{\delta\hat{U}^\dagger(t,-\infty)}{\delta B(t')} &= \mathrm{i}\hat{U}^\dagger(t',-\infty)\sum_{\boldsymbol{k}}\varepsilon(\boldsymbol{k}-e\boldsymbol{A}(t'))\hat{n}^d_{\boldsymbol{k}}\hat{U}^\dagger(t,t').\end{aligned} \tag{28}$$

After substituting these expressions into the equation for the functional derivative of the average of the stress tensor operator, we find that it is equal to the average of the commutator of the stress tensor operators at different times,

$$\begin{aligned}\frac{\delta\langle\hat{\gamma}(t)\rangle}{\delta B(t')} &= -\frac{1}{Z}\mathrm{Tr}\left\{\mathrm{e}^{-\beta\hat{\mathcal{H}}_{\rm FK}}\sum_{\boldsymbol{k}}\varepsilon(\boldsymbol{k}-e\boldsymbol{A}(t))\left(\mathrm{i}\hat{U}^\dagger(t',-\infty)\sum_{\boldsymbol{k}'}\varepsilon(\boldsymbol{k}'-e\boldsymbol{A}(t'))\hat{n}^d_{\boldsymbol{k}'}\hat{U}^\dagger(t,t')\hat{n}^d_{\boldsymbol{k}}\hat{U}(t,-\infty)\right.\right.\\ &\quad\left.\left.-\,\mathrm{i}\hat{U}^\dagger(t,-\infty)\hat{n}^d_{\boldsymbol{k}}\hat{U}(t,t')\sum_{\boldsymbol{k}'}\varepsilon(\boldsymbol{k}'-e\boldsymbol{A}(t'))\hat{n}^d_{\boldsymbol{k}'}\hat{U}(t',-\infty)\right)\right\}_{\theta(t'<t)}\\ &= -\frac{1}{Z}\mathrm{Tr}\left\{\mathrm{e}^{-\beta\hat{\mathcal{H}}_{\rm FK}}\left(\mathrm{i}\sum_{\boldsymbol{k}'}\varepsilon(\boldsymbol{k}'-e\boldsymbol{A}(t'))\hat{U}^\dagger(t',-\infty)\hat{n}^d_{\boldsymbol{k}'}\hat{U}(t',-\infty)\sum_{\boldsymbol{k}}\varepsilon(\boldsymbol{k}-e\boldsymbol{A}(t))\hat{U}^\dagger(t,-\infty)\hat{n}^d_{\boldsymbol{k}}\hat{U}(t,-\infty)\right.\right.\\ &\quad\left.\left.-\,\mathrm{i}\sum_{\boldsymbol{k}}\varepsilon(\boldsymbol{k}-e\boldsymbol{A}(t))\hat{U}^\dagger(t,-\infty)\hat{n}^d_{\boldsymbol{k}}\hat{U}(t,-\infty)\sum_{\boldsymbol{k}'}\varepsilon(\boldsymbol{k}'-e\boldsymbol{A}(t'))\hat{U}^\dagger(t',-\infty)\hat{n}^d_{\boldsymbol{k}'}\hat{U}(t',-\infty)\right)\right\}_{\theta(t'<t)}\\ &= \mathrm{i}\frac{1}{Z}\mathrm{Tr}\{\mathrm{e}^{-\beta\hat{\mathcal{H}}_{\rm FK}}(\hat{\gamma}(t)\hat{\gamma}(t')-\hat{\gamma}(t')\hat{\gamma}(t))\}_{\theta(t'<t)} = \mathrm{i}\langle[\hat{\gamma}(t),\hat{\gamma}(t')]\rangle_{\theta(t'<t)},\end{aligned} \tag{29}$$

which is the nonresonant Raman scattering response function.

In equilibrium, the nonresonant Raman scattering response function is connected to the nonresonant Raman scattering cross section by the Bose-Einstein distribution function

$$\chi_{\rm N}(\Omega) = R_{\rm N}(\Omega)(\mathrm{e}^{\beta\Omega}-1), \tag{30}$$

where $\Omega=\omega_i-\omega_f$ is a difference between the frequencies of incident and scattered light. Instead, in nonequilibrium there is no such a connection and we have to calculate the Raman scattering cross section directly. According to Eq. (20), the cross section is found from the greater Green's function built on the two stress tensor operators at different times,

$$R_{\rm N}(t,t') = R^{>}(t,t') = \langle\hat{\gamma}(t)\hat{\gamma}(t')\rangle. \tag{31}$$

The greater Green's function corresponds to the case when time t belongs to the lower branch and time t' to the upper branch of the Kadanoff-Baym-Keldysh contour in Fig. 1. In our numerical calculation of the average of the stress tensor operator $\langle\hat{\gamma}(t)\rangle_{B(t)}$ with the field $B(t)$ applied, we are actually able to choose where to apply this field. If we apply it on the whole contour, then both terms in the parentheses in Eq. (27) contribute to the functional derivative, which results in the commutator of two γ operators (retarded correlation function) in Eq. (29). Otherwise, if we apply it only on the upper or lower branch of the contour, then only one term in Eq. (27) contributes, which results in the product of the two γ operators (either greater or lesser correlation functions) in Eq. (29). Hence, both the Raman scattering cross section and the response function are formally defined in a similar way via functional derivatives of the average of the stress tensor operator, but the numerical calculation of each of these is different. For the A_{1g} symmetry channel, the incident and scattered light are polarized along each coordinate axis, and then added over all axes. This gives us the expression for the nonresonant Raman scattering cross section in terms of the functional derivative for the A_{1g} symmetry channel to be

$$R^{A_{1g}}_{\rm N}(t,t') = -\frac{\delta\langle\hat{\gamma}(t)\rangle}{\delta B(t')} = -\lim_{\delta B\to 0}\frac{\langle\hat{\gamma}(t)\rangle_{B(t)}-\langle\hat{\gamma}(t)\rangle}{\delta B(t')}. \tag{32}$$

Further Fourier transform to the frequency domain results in the final expression for the Raman scattering cross section, which is

$$R^{A_{1g}}_{\rm N}(\omega,t_p) = \frac{1}{\pi}\int\mathrm{d}t\int\mathrm{d}t' s(t,t_p)s(t',t_p)\mathrm{e}^{-\mathrm{i}\omega(t-t')}R^{A_{1g}}_{\rm N}(t,t'), \tag{33}$$

with the same probe pulse envelope function $s(t,t_p)$ as in Eqs. (18) and (20).

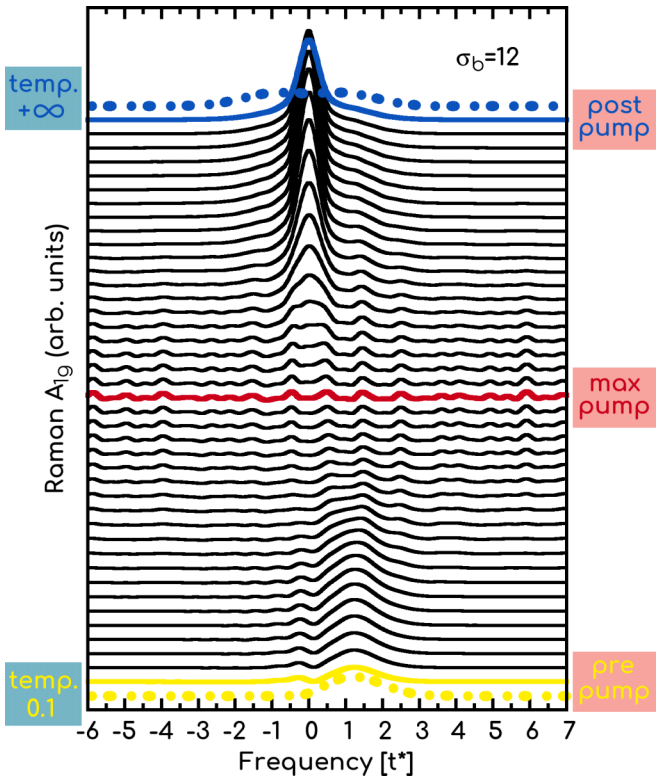


FIG. 2. Waterfall plot for the Raman scattering cross section for in case of a bad metal phase in equilibrium with Coulomb interaction $U = 1$. Dotted lines correspond to the equilibrium results at temperatures $T = 0.1$ (yellow) and $T \to \infty$ (blue). Different lines correspond to different time delays t_p of the probe pulse with respect to the pump pulse with $t_p \in [-20, 20]$, starting from times before the pump (yellow line) to the time with the maximum pump (red line) and to the late times after the pump pulse is gone (blue line). Stokes and anti-Stokes peaks are centered around frequencies $\omega = U$ and $\omega = -U$, respectively. The peak at zero frequency corresponds to the elastic contribution to the scattering cross section. The probe pulse width is given by $\sigma_b = 12$.

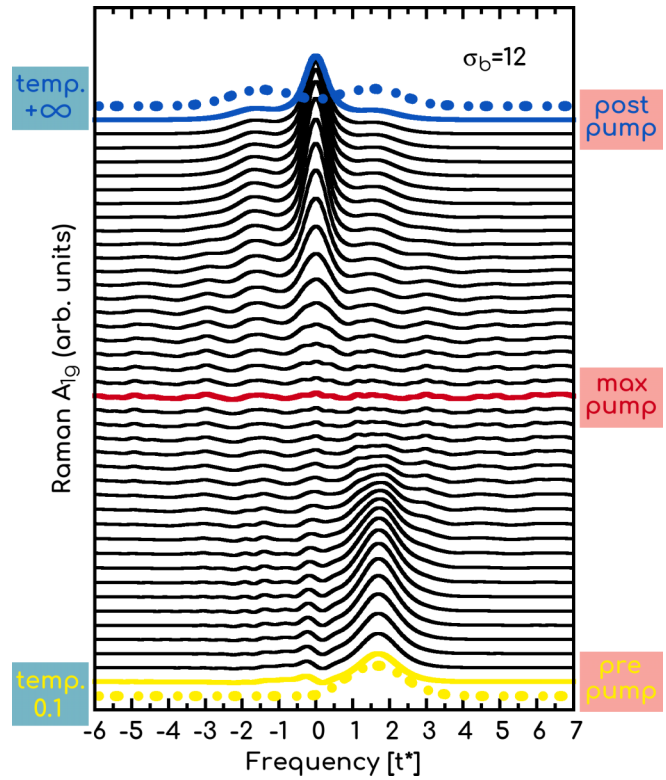


FIG. 3. Similar to Fig. 2, this is a waterfall plot for the Raman scattering cross section in the case of a near-critical metal-Mott-insulator transition in equilibrium with Coulomb interaction $U = 1.5$.

III. RESULTS

We present our results for the nonresonant Raman scattering cross section in the A_{1g} symmetry channel. We solve it for the Falicov-Kimball model, which can be solved exactly within the dynamical mean-field theory. We do not present here the details on how we calculate the appropriate single-particle Green's functions needed to determine the average of the stress tensor operator as it is fully described in series of our previous papers [37,38]. Instead, we aim to demonstrate the power and applicability of the method to a complex problem that is extremely hard to solve analytically. We examine metallic, near critical to metal-insulator transition, and Mott insulator phases, which correspond to the Coulomb interactions $U = 1$, $U = 1.5$, and $U = 2$, respectively.

In Fig. 2, we present the results for the nonresonant Raman scattering cross section in the case of a bad metal phase with Coulomb interaction $U = 1$. The waterfall-like plots demonstrate the evolution of the cross section in time. Every line corresponds to different delay times t_p of the probe pulse with respect to the pump pulse. The yellow line corresponds to early times, when the system was in equilibrium, which has a single peak centered around the value of interaction U. The pump field suppresses the Raman signal until it disappears completely near the time of the maximum of the pump, which corresponds to the red line. After the pump is gone, the Raman signal recovers with a peak at $\omega = U$, but the dominant peak is now at zero frequency (which corresponds to the elastic contribution) as indicated with the blue line. The system does not reach the high-temperature regime, where one expects all peaks to be equal in weight. These results are similar to the results for the B_{1g} symmetry channel which we calculated with an analytical formula [34], but the magnitude is much smaller because the A_{1g} channel has the same symmetry as the lattice, which allows the signal to be screened. This comparison also serves as a good confirmation of the reliability of our results.

In Fig. 3 we show results for the case of a near-critical metal-Mott-insulator transition with Coulomb interaction $U = 1.5$. In this case, we observe similar behavior as for the metal, except that the anti-Stokes line starts to develop immediately after the pump and at later times becomes larger than the Stokes one. This scenario corresponds to an inverse occupation of the states arising from a negative effective temperature. This behavior is also present in the case of the B_{1g} symmetry channel.

In Fig. 4, we show the results for the case of a Mott insulator with a Coulomb interaction $U = 2$. In this case, the Raman scattering cross section at late times after the pump pulse is gone has the Stokes peak recovered, a zero-frequency

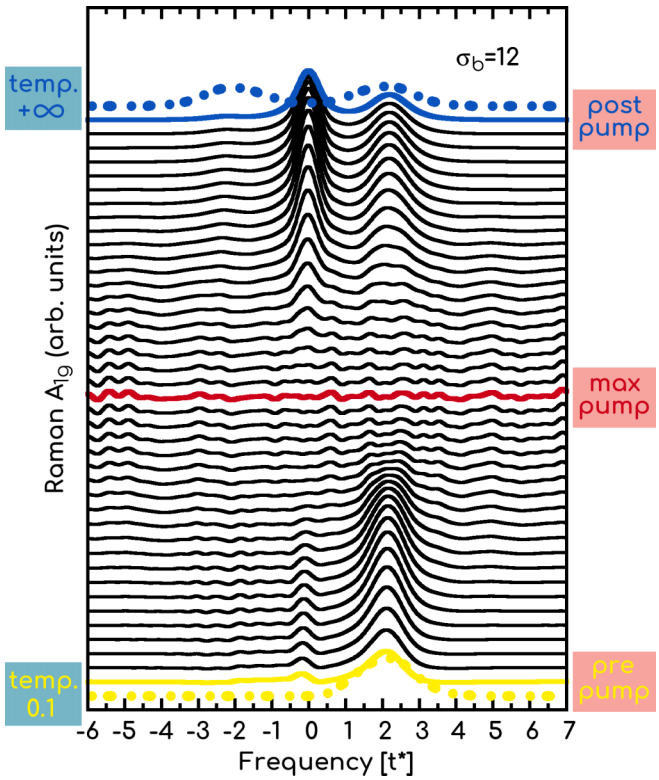


FIG. 4. Similar to the Fig. 2, waterfall plot for the Raman scattering cross section in the case of a Mott insulator in equilibrium with a Coulomb interaction $U = 2$.

peak, and a slightly developed anti-Stokes peak, which is more similar to the behavior in the metallic phase, than in the case of the near-critical transition. This is also similar to what we saw in the B_{1g} results.

In summary, the behavior we see in the A_{1g} channel is similar to what we saw in the B_{1g} channel, but reduced in magnitude due to the screening from the vertex corrections. The metallic and Mott-insulating phases have their energy raised to an effective temperature that is high, but well below infinity, while the near-critical phase has its effective temperature raised past infinity to a negative temperature. In all cases, we see the development from an initial equilibrium response to a dead region during the pulse, which then recovers to a much higher-temperature response. The functional derivative method used here includes all vertex correction effects and, because it involves just a single functional derivative, it is feasible to calculate it.

IV. CONCLUSIONS

In this paper, we developed the functional derivative method for calculating the Raman cross section in nonequilibrium. We evaluated results for the Falicov-Kimball model in the A_{1g} symmetry channel. This result demonstrates that the functional derivative approach works and that it serves as a powerful tool for solving complex problems in the theory of the strongly correlated systems out of the equilibrium. Our results show the importance of applying the functional derivative on the lattice rather than to the impurity problem in the DMFT solution. In this way, one recovers the proper zero-momentum response function.

A striking result seen here, as in other symmetry channels, is that the pump pulse appears to make the Raman response vanish. It is not clear what the mechanism is that does this, but the deadening of the response when the pump is near its maximum is a striking result that we see in these data. A clear explanation for why this is occurring remains to be worked out.

ACKNOWLEDGMENTS

This work was supported by the U.S. Department of Energy, Office of Basic Energy Sciences, Division of Materials Sciences and Engineering, under Grant No. DE-FG02-08ER46542. This research used resources of the National Energy Research Scientific Computing Center (NERSC), a Department of Energy User Facility using NERSC Award No. BES-ERCAP 41865. J.K.F. was also supported by the McDevitt bequest at Georgetown University.

DATA AVAILABILITY

The data that support the findings of this article are openly available [39].

APPENDIX: OPTICAL CONDUCTIVITY APPROACH

Similar to the Raman scattering, we may also develop a functional derivative approach for the optical conductivity in nonequilibrium. Here, we use the same notations as in the main text, unless otherwise defined. We start from the general definition of the optical conductivity that relates the induced charge current to the applied electric field and in the time domain it can be written as follows,

$$-e\langle \hat{j}_a(t)\rangle = \sum_b \int_{-\infty}^{t} \mathrm{d}\bar{t}\,\sigma_{a,b}(t,\bar{t})\left(-\frac{\partial A_b(\bar{t})}{\partial \bar{t}}\right), \tag{A1}$$

where $\hat{j}_a(t)$ is the current operator defined in Eq. (12) (in the main text) and the electric field has been replaced by the vector potential [Eq. (5) in main text]. Taking the functional derivative of this expression with respect to the vector potential (at a second time) results in

$$-e\frac{\delta\langle \hat{j}_a(t)\rangle}{\delta A_b(t')} = \frac{\partial}{\partial t'}\sigma_{a,b}(t,t'), \tag{A2}$$

because the optical conductivity $\sigma_{a,b}(t,t')$ does not depend on the vector potential (since it is a property of the material only). Note that we used an integration by parts to move the derivative onto the optical conductivity term. This is not a derivation, so it is actually the definition of the optical conductivity. Next, we determine how to compute this expression directly in our many-body formalism. Similar to the stress tensor operator in Eqs. (22) and (23) (in the main text), for the charge current, we have

$$-e\langle \hat{j}_a(t)\rangle = \mathrm{i}e\sum_{\boldsymbol{k},\sigma} v_a(\boldsymbol{k}-e\boldsymbol{A}(t))G^{<}_{\boldsymbol{k},\sigma}(t,t), \tag{A3}$$

where the electron velocity is $v_a(\boldsymbol{k}-e\boldsymbol{A}(t)) = \partial\varepsilon(\boldsymbol{k}-e\boldsymbol{A}(t))/\partial k_a$. Taking the functional derivative of this expression

for the charge current with respect to the vector potential $A_b(t')$ results in two terms coming from the vector-potential dependence in the Green's function and in the electron velocity:

$$-e\frac{\delta\langle\hat{j}_a(t)\rangle}{\delta A_b(t')} = \mathrm{i}e\sum_{\boldsymbol{k},\sigma}\left[\frac{\delta G^<_{\boldsymbol{k},\sigma}(t,t)}{\delta A_b(t')}v_a(\boldsymbol{k}-e\boldsymbol{A}(t)) + G^<_{\boldsymbol{k},\sigma}(t,t)\sum_{b'}\frac{\partial v_a(\boldsymbol{k}-e\boldsymbol{A}(t))}{\partial k_{b'}}\frac{\delta(-eA_{b'}(t))}{\delta A_b(t')}\right]. \tag{A4}$$

For the case of the hypercubic lattice with nearest-neighbor hopping only, the derivative of the velocity with respect to momentum then results in the same band-structure term multiplied by -1, as follows:

$$\frac{\partial v_a(\boldsymbol{k}-e\boldsymbol{A}(t))}{\partial k_b} = \frac{\partial^2\varepsilon(\boldsymbol{k}-e\boldsymbol{A}(t))}{\partial k_b\partial k_a} = -\varepsilon(\boldsymbol{k}-e\boldsymbol{A}(t))\delta_{a,b}. \tag{A5}$$

Consequently, the second term in Eq. (A4) is the negative of the kinetic energy. For the first term in Eq. (A4), all the dependence on the vector potential $\boldsymbol{A}(t)$ in the lesser Green's function comes through the evolution operators $\hat{U}(t,t_0) = \mathcal{T}_t\exp\left[-\mathrm{i}\int_{t_0}^t \mathrm{d}\bar{t}\,\tilde{\hat{\mathcal{H}}}(\bar{t})\right]$ (and its Hermitian conjugate) that appear on either side of the creation and annihilation operators in the Heisenberg picture $\hat{c}^{(\dagger)}_{k,\sigma}(t) = \hat{U}^\dagger(t,t_0)\hat{c}^{(\dagger)}_{k,\sigma}\hat{U}(t,t_0)$. The functional derivative of the evolution operator is found by locating precisely where $A_b(t')$ appears in the time-ordered product, and computing the derivative with respect to it. We have

$$\begin{aligned}\frac{\delta\hat{U}(t,t_0)}{\delta A_b(t')} &= \frac{\delta}{\delta A_b(t')}\mathcal{T}_t\mathrm{e}^{-\mathrm{i}\left(\int_{t_0}^{t'-\Delta(\to 0)}\mathrm{d}\bar{t}\,\tilde{\hat{\mathcal{H}}}(\bar{t})+\int_{t'}^{t}\mathrm{d}\bar{t}\,\tilde{\hat{\mathcal{H}}}(\bar{t})\right)}\\ &= \mathcal{T}_t\left\{-\mathrm{i}\mathrm{e}^{-\mathrm{i}\int_{t'}^t\mathrm{d}\bar{t}\,\tilde{\hat{\mathcal{H}}}(\bar{t})}\int_{t'}^t\mathrm{d}\bar{t}\frac{\delta\tilde{\hat{\mathcal{H}}}(\bar{t})}{\delta A_b(t')}\mathrm{e}^{-\mathrm{i}\int_{t_0}^{t'-\Delta}\mathrm{d}\bar{t}\,\tilde{\hat{\mathcal{H}}}(\bar{t})}\right\}\theta(t'<t)\\ &= \hat{U}(t,t')\mathrm{i}e\sum_{\boldsymbol{k},\sigma}v_b(\boldsymbol{k}-e\boldsymbol{A}(t'))\hat{c}^\dagger_{\boldsymbol{k},\sigma}\hat{c}_{\boldsymbol{k},\sigma}\hat{U}(t',t_0)\theta(t'<t),\end{aligned} \tag{A6}$$

under the assumption that the potential energy is independent of the vector potential. Note that the functional derivative of the Hamiltonian is found from Eq. (7) (in the main text) to be equal to

$$\frac{\delta\tilde{\hat{\mathcal{H}}}(t)}{\delta A_b(t')} = -e\sum_{\boldsymbol{k},\sigma}v_b(\boldsymbol{k}-e\boldsymbol{A}(t))\delta(t-t')\hat{c}^\dagger_{\boldsymbol{k},\sigma}\hat{c}_{\boldsymbol{k},\sigma}, \tag{A7}$$

and we use this result in the above derivation.

Now we can compute the functional derivative of the product of the creation and annihilation operators at the same time, which appear in the formula for the charge current, producing

$$\begin{aligned}\frac{\delta\,\hat{c}^\dagger_{\boldsymbol{k},\sigma}(t)\hat{c}_{\boldsymbol{k},\sigma}(t)}{\delta A_b(t')} &= \frac{\delta\hat{U}^\dagger(t,t_0)}{\delta A_b(t')}\hat{c}^\dagger_{\boldsymbol{k},\sigma}\hat{c}_{\boldsymbol{k},\sigma}\hat{U}(t,t_0) + \hat{U}^\dagger(t,t_0)\hat{c}^\dagger_{\boldsymbol{k},\sigma}\hat{c}_{\boldsymbol{k},\sigma}\frac{\delta\hat{U}(t,t_0)}{\delta A_b(t')}\\ &= -\mathrm{i}e\hat{U}^\dagger(t',t_0)\sum_{\bar{\boldsymbol{k}},\bar{\sigma}}v_b(\bar{\boldsymbol{k}}-e\boldsymbol{A}(t'))\\ &\quad\times\hat{c}^\dagger_{\bar{\boldsymbol{k}},\bar{\sigma}}\hat{c}_{\bar{\boldsymbol{k}},\bar{\sigma}}\hat{U}^\dagger(t,t')\hat{c}^\dagger_{\boldsymbol{k},\sigma}\hat{c}_{\boldsymbol{k},\sigma}\hat{U}(t,t_0)\\ &\quad+\mathrm{i}e\hat{U}^\dagger(t,t_0)\hat{c}^\dagger_{\boldsymbol{k},\sigma}\hat{c}_{\boldsymbol{k},\sigma}\hat{U}(t,t')\\ &\quad\times\sum_{\bar{\boldsymbol{k}},\bar{\sigma}}v_b(\bar{\boldsymbol{k}}-e\boldsymbol{A}(t'))\hat{c}^\dagger_{\bar{\boldsymbol{k}},\bar{\sigma}}\hat{c}_{\bar{\boldsymbol{k}},\bar{\sigma}}\hat{U}(t',t_0)\\ &= \mathrm{i}e[\hat{c}^\dagger_{\boldsymbol{k},\sigma}(t)\hat{c}_{\boldsymbol{k},\sigma}(t),\hat{j}_b(t')]\theta(t'<t).\end{aligned} \tag{A8}$$

Note how this creates a commutator from the derivative acting on the upper and lower branches of the contour and how the Heaviside function enters because if $t<t'$ then we have no commutator and the two terms cancel. Substituting this result into the expression for the functional derivative of the current in Eq. (A4) and using Eq. (A2), we find the expression for the two-time optical conductivity is given by

$$\begin{aligned}\frac{\partial}{\partial t'}\sigma_{a,b}(t,t') &= -e\frac{\delta\langle\hat{j}_a(t)\rangle}{\delta A_b(t')}\\ &= \mathrm{i}e^2\langle[\hat{j}_a(t),\hat{j}_b(t')]\rangle_{\theta(t'<t)}\\ &\quad+e^2\langle\hat{T}(t)\rangle\delta(t-t')\delta_{a,b},\end{aligned} \tag{A9}$$

where the average kinetic energy term is $\langle\hat{T}\rangle = -\mathrm{i}\sum_{\boldsymbol{k},\sigma}\varepsilon(\boldsymbol{k}-e\boldsymbol{A}(t))G^<_{\boldsymbol{k},\sigma}(t,t)$. We reiterate again that the commutator and the θ function arise from the derivative of the evolution operator on both the upper $\hat{U}$ and lower $\hat{U}^\dagger$ branches, which cancels if $t'>t$ and gives a commutator if $t'<t$.

To find the frequency-dependent optical conductivity, we use Wigner coordinates, with average $t_{\mathrm{ave}} = (t+t')/2$ and relative $t_{\mathrm{rel}} = t-t'$ times. This representation allows us to Fourier transform the optical conductivity with respect to the relative time for each average time

$$\sigma_{a,b}(t_{\mathrm{ave}},\omega) = \int_{-\infty}^{+\infty}\mathrm{d}t_{\mathrm{rel}}\mathrm{e}^{\mathrm{i}\omega t_{\mathrm{rel}}}\sigma_{a,b}\left(t_{\mathrm{ave}}+\frac{t_{\mathrm{rel}}}{2},t_{\mathrm{ave}}-\frac{t_{\mathrm{rel}}}{2}\right). \tag{A10}$$

Defining the partial time derivative in terms of new variables as $\frac{\partial}{\partial t'} = \frac{\partial}{2\partial t_{\mathrm{ave}}} - \frac{\partial}{\partial t_{\mathrm{rel}}}$, we rewrite Eq. (A9) after the Fourier transformation as

$$\begin{aligned}&\int_{-\infty}^{+\infty}\mathrm{d}t_{\mathrm{rel}}\mathrm{e}^{\mathrm{i}\omega t_{\mathrm{rel}}}\left(\frac{\partial}{2\partial t_{\mathrm{ave}}}-\frac{\partial}{\partial t_{\mathrm{rel}}}\right)\sigma_{a,b}(t_{\mathrm{ave}},t_{\mathrm{rel}})\\ &= \left(\frac{\partial}{2\partial t_{\mathrm{ave}}}+\mathrm{i}\omega\right)\sigma_{a,b}(t_{\mathrm{ave}},\omega)\\ &= -e\int_{-\infty}^{+\infty}\mathrm{d}t_{\mathrm{rel}}\mathrm{e}^{\mathrm{i}\omega t_{\mathrm{rel}}}\frac{\delta\left\langle\hat{j}_a\left(t_{\mathrm{ave}}+\frac{t_{\mathrm{rel}}}{2}\right)\right\rangle}{\delta A_b\left(t_{\mathrm{ave}}-\frac{t_{\mathrm{rel}}}{2}\right)}\\ &= \int_{-\infty}^{+\infty}\mathrm{d}t_{\mathrm{rel}}\mathrm{e}^{\mathrm{i}\omega t_{\mathrm{rel}}}\mathrm{i}e^2\left\langle\left[\hat{j}_a\left(t_{\mathrm{ave}}+\frac{t_{\mathrm{rel}}}{2}\right),\hat{j}_b\left(t_{\mathrm{ave}}-\frac{t_{\mathrm{rel}}}{2}\right)\right]\right\rangle\\ &\quad+e^2\langle T(t_{\mathrm{ave}})\rangle\delta_{ab}.\end{aligned} \tag{A11}$$

Defining the nonequilibrium two-time-dependent retarded current-current correlation function as $\Pi^{jj}_{a,b}(t,t') = -\mathrm{i}\theta(t-$

$t'\rangle\langle[\hat{j}_a(t), \hat{j}_b(t')]\rangle$, we obtain the equation for the nonequilibrium frequency-dependent optical conductivity as follows:

$$\left[\frac{1}{2}\partial_{t_{\rm ave}} + \mathrm{i}\omega\right]\sigma_{a,b}(t_{\rm ave}, \omega) = -e^2\int_0^{+\infty} \mathrm{d}t_{\rm rel}\mathrm{e}^{\mathrm{i}\omega t_{\rm rel}}\Pi^{jj}_{a,b}\left(t_{\rm ave} + \frac{t_{\rm rel}}{2}, t_{\rm ave} - \frac{t_{\rm rel}}{2}\right) + e^2\langle\hat{T}(t_{\rm ave})\rangle\delta_{a,b}. \tag{A12}$$

As a check of this derivation, we compare it to the equilibrium result. In this case, there is no dependence on $t_{\rm ave}$ and Eq. (A12) becomes equal to

$$\sigma_{a,b}(\omega) = \mathrm{i}e^2\frac{\Pi^{jj}_{a,b}(\omega) - \langle\hat{T}\rangle\delta_{a,b}}{\omega}, \tag{A13}$$

which corresponds to the result of the Kubo linear-response approach [40,41]. There is an additional complication in the nonequilibrium case, whereby we need to solve the extra differential equation in average time to find the nonequilibrium optical conductivity

$$\left[\frac{\partial}{2\partial_{t_{\rm ave}}} + \mathrm{i}\omega\right]\sigma_{a,b}(t_{\rm ave}, \omega) = -e^2\Pi^{jj}_{a,b}(t_{\rm ave}, \omega) + e^2\langle\hat{T}(t_{\rm ave})\rangle\delta_{a,b}, \tag{A14}$$

where $\Pi^{jj}_{a,b}(t_{\rm ave}, \omega)$ is the Fourier transform of the current-current correlation function in Eq. (A12). Numerically, we can calculate the right-hand side of this equation by shifting the vector potential $A(t)$ by a small amount $\delta A(t)$ [$A(t) \to A(t) + \delta A(t)$] and taking the numerical functional derivative with respect to this shift, as it follows from Eq. (A9).

In the case of the infinite-dimensional hypercubic lattice, we assume that the vector potential is directed along the main diagonal of the lattice, but in the case of lower dimensions one has to track spatial indices carefully in order to add the perturbation properly, depending on the direction of the field. With this approach we avoid the calculation of the vertex corrections, but instead deal with accuracy issues associated with the calculation of numerical derivatives by finite differences. The kinetic energy term, that contributes to the functional derivative, will vanish if we take only the real part for the optical conductivity. The first-order differential equation should be able to be solved directly. We are not aware of any work that has properly evaluated this final result yet.

Unfortunately, we cannot provide an expression for the time-resolved optical conductivity spectra. In equilibrium, such spectra are extracted from the reflectivity measurements through the Kramers-Kronig relations and requires knowledge of the refractive indices, which are both unknown for the nonequilibrium case of the pump-probe experiments. In fact, while it is relatively easy for theorists to calculate the optical conductivity and for experimentalists to measure the reflectivity, the connection between these two results has not yet been worked out in nonequilibrium. It is complicated—in equilibrium it requires a Kramers-Kronig analysis that uses properties of the plasmon. In nonequilibrium, the precise way to make this connection is not known.

[1] F. Rossi and T. Kuhn, Theory of ultrafast phenomena in photoexcited semiconductors, Rev. Mod. Phys. **74**, 895 (2002).

[2] G. Claudio, C. Massimo, F. Daniele, F. Michele, P. Fulvio, and M. Dragan, Ultrafast optical spectroscopy of strongly correlated materials and high-temperature superconductors: A non-equilibrium approach, Adv. Phys. **65**, 58 (2016).

[3] D. N. Basov, R. D. Averitt, and D. Hsieh, Towards properties on demand in quantum materials, Nat. Mater. **16**, 1077 (2017).

[4] A. de la Torre, D. M. Kennes, M. Claassen, S. Gerber, J. W. McIver, and M. A. Sentef, Colloquium: Nonthermal pathways to ultrafast control in quantum materials, Rev. Mod. Phys. **93**, 041002 (2021).

[5] D. Wegkamp, M. Herzog, L. Xian, M. Gatti, P. Cudazzo, C. L. McGahan, R. E. Marvel, R. F. Haglund, A. Rubio, M. Wolf, and J. Stähler, Instantaneous band gap collapse in photoexcited monoclinic VO_2 due to photocarrier doping, Phys. Rev. Lett. **113**, 216401 (2014).

[6] D. Hsieh, F. Mahmood, D. H. Torchinsky, G. Cao, and N. Gedik, Observation of a metal-to-insulator transition with both Mott-Hubbard and Slater characteristics in Sr_2IrO_4 from time-resolved photocarrier dynamics, Phys. Rev. B **86**, 035128 (2012).

[7] S. Iwai, M. Ono, A. Maeda, H. Matsuzaki, H. Kishida, H. Okamoto, and Y. Tokura, Ultrafast optical switching to a metallic state by photoinduced Mott transition in a halogen-bridged nickel-chain compound, Phys. Rev. Lett. **91**, 057401 (2003).

[8] A. Cavalleri, T. Dekorsy, H. H. W. Chong, J. C. Kieffer, and R. W. Schoenlein, Evidence for a structurally-driven insulator-to-metal transition in VO_2: A view from the ultrafast timescale, Phys. Rev. B **70**, 161102(R) (2004).

[9] H. Okamoto, H. Matsuzaki, T. Wakabayashi, Y. Takahashi, and T. Hasegawa, Photoinduced metallic state mediated by spin-charge separation in a one-dimensional organic Mott insulator, Phys. Rev. Lett. **98**, 037401 (2007).

[10] F. Schmitt, P. S. Kirchmann, U. Bovensiepen, R. G. Moore, L. Rettig, M. Krenz, J.-H. Chu, N. Ru, L. Perfetti, D. H. Lu, M. Wolf, I. R. Fisher, and Z.-X. Shen, Transient electronic structure and melting of a charge density wave in $TbTe_3$, Science **321**, 1649 (2008).

[11] L. Perfetti, P. A. Loukakos, M. Lisowski, U. Bovensiepen, M. Wolf, H. Berger, S. Biermann, and A. Georges, Femtosecond dynamics of electronic states in the Mott insulator 1T-TaS_2 by time resolved photoelectron spectroscopy, New J. Phys. **10**, 053019 (2008).

[12] S. Hellmann, M. Beye, C. Sohrt, T. Rohwer, F. Sorgenfrei, H. Redlin, M. Kalläne, M. Marczynski-Bühlow, F. Hennies, M. Bauer, A. Föhlisch, L. Kipp, W. Wurth, and K. Rossnagel, Ultrafast melting of a charge-density wave in the Mott insulator 1T-TaS_2, Phys. Rev. Lett. **105**, 187401 (2010).

[13] J. Graf, C. Jozwiak, C. L. Smallwood, H. Eisaki, R. A. Kaindl, D.-H. Lee, and A. Lanzara, Nodal quasiparticle meltdown in ultrahigh-resolution pump-probe angle-resolved photoemission, Nat. Phys. **7**, 805 (2011).

[14] D. Fausti, R. I. Tobey, N. Dean, S. Kaiser, A. Dienst, M. C. Hoffmann, S. Pyon, T. Takayama, H. Takagi, and A. Cavalleri, Light-induced superconductivity in a stripe-ordered cuprate, Science **331**, 189 (2011).

[15] W. Hu, S. Kaiser, D. Nicoletti, C. R. Hunt, I. Gierz, M. C. Hoffmann, M. Le Tacon, T. Loew, B. Keimer, and A. Cavalleri, Optically enhanced coherent transport in $YBa_2Cu_3O_{6.5}$ by ultrafast redistribution of interlayer coupling, Nat. Mater. **13**, 705 (2014).

[16] M. Mitrano, A. Cantaluppi, D. Nicoletti, S. Kaiser, A. Perucchi, S. Lupi, D. Di Pietro, P. Pontiroli, M. Riccò, S. R. Clark, D. Jaksch, and A. Cavalleri, Possible light-induced superconductivity in K_3C_{60} at high temperature, Nature (London) **530**, 461 (2016).

[17] T. P. Devereaux and R. Hackl, Inelastic light scattering from correlated electrons, Rev. Mod. Phys. **79**, 175 (2007).

[18] Luuk J. P. Ament, M. van Veenendaal, T. P. Devereaux, J. P. Hill, and J. van den Brink, Resonant inelastic x-ray scattering studies of elementary excitations, Rev. Mod. Phys. **83**, 705 (2011).

[19] L. P. Kadanoff and G. Baym, *Quantum Statistical Mechanics* (W. A. Benjamin, New York, 1962).

[20] L. V. Keldysh, Diagram technique for nonequilibrium processes, Zh. Eksp. Teor. Fiz. **47**, 1515 (1964) [Sov. Phys. JETP **20**, 1018 (1965)].

[21] G. Stefanucci and R. van Leeuwen, *Nonequilibrium Many-Body Theory of Quantum Systems* (Cambridge University Press, New York, 2013).

[22] G. Baym and L. P. Kadanoff, Conservation laws and correlation functions, Phys. Rev. **124**, 287 (1961).

[23] G. Baym, Self-consistent approximations in many-body systems, Phys. Rev. **127**, 1391 (1962).

[24] N.-H. Kwong and M. Bonitz, Real-time Kadanoff-Baym approach to plasma oscillations in a correlated electron gas, Phys. Rev. Lett. **84**, 1768 (2000).

[25] N. Säkkinen, M. Manninen, and R. van Leeuwen, The Kadanoff–Baym approach to double excitations in finite systems, New J. Phys. **14**, 013032 (2012).

[26] M. Eckstein and P. Werner, Simulation of time-dependent resonant inelastic x-ray scattering using nonequilibrium dynamical mean-field theory, Phys. Rev. B **103**, 115136 (2021).

[27] P. Werner, S. Johnston, and M. Eckstein, Nonequilibrium-DMFT based RIXS investigation of the two-orbital Hubbard model, Europhys. Lett. **133**, 57005 (2021).

[28] P. Werner and M. Eckstein, Nonequilibrium resonant inelastic x-ray scattering study of an electron-phonon model, Phys. Rev. B **104**, 085155 (2021).

[29] P. Werner, F. Petocchi, and M. Eckstein, Time-resolved photoemission and resonant inelastic x-ray scattering study of a site-selective Mott insulator, Phys. Rev. B **107**, 035157 (2023).

[30] P. Werner, M. Eckstein, and N. Tsuji, Nonequilibrium DMFT approach to time-resolved Raman spectroscopy, Phys. Rev. B **108**, 245157 (2023).

[31] J. K. Freericks and T. P. Devereaux, Non-resonant Raman scattering through a metal-insulator transition: An exact analysis of the Falicov-Kimball model, Condens. Matter Phys. **4**, 149 (2001).

[32] J. K. Freericks and T. P. Devereaux, Raman scattering through a metal-insulator transition, Phys. Rev. B **64**, 125110 (2001).

[33] A. M. Shvaika, O. Vorobyov, J. K. Freericks, and T. P. Devereaux, Electronic Raman scattering in correlated materials: A treatment of nonresonant, mixed, and resonant scattering using dynamical mean-field theory, Phys. Rev. B **71**, 045120 (2005).

[34] O. P. Matveev, A. M. Shvaika, T. P. Devereaux, and J. K. Freericks, Stroboscopic tests for thermalization of electrons in pump-probe experiments, Phys. Rev. Lett. **122**, 247402 (2019).

[35] L. M. Falicov and J. C. Kimball, Simple model for semiconductor-metal transitions: SmB_6 and transition-metal oxides, Phys. Rev. Lett. **22**, 997 (1969).

[36] J. K. Freericks, V. M. Turkowski, and V. Zlatić, Nonequilibrium dynamical mean-field theory, Phys. Rev. Lett. **97**, 266408 (2006).

[37] V. Turkowski and J. K. Freericks, Nonlinear response of Bloch electrons in infinite dimensions, Phys. Rev. B **71**, 085104 (2005).

[38] J. K. Freericks, Quenching Bloch oscillations in a strongly correlated material: Nonequilibrium dynamical mean-field theory, Phys. Rev. B **77**, 075109 (2008).

[39] O. Matveev, Nonequilibrium Raman scattering cross-section in the A_{1g} symmetry channel for the Falicov-Kimball model with DMFT [Data set], Zenodo (2025), https://doi.org/10.5281/zenodo.16540704.

[40] R. Kubo, Statistical-mechanical theory of irreversible processes. I. General theory and simple applications to magnetic and conduction problems, J. Phys. Soc. Jpn. **12**, 570 (1957).

[41] G. D. Mahan, *Many-Particle Physics*, 3rd ed., Physics of Solids and Liquids (Springer, New York, 2000).

Correction: A funding statement was missing from the Acknowledgments and has been inserted.